Asymmetric orientational writing in glass with femtosecond laser irradiation

Bertrand Poumellec, M. Lancry, R. Desmarchelier, Eveline Hervé, François Brisset, J.C. Poulin

Asymmetric Orientational Writing in glass with femtosecond laser irradiation

B. Poumellec,[1] M. Lancry[1] R. Desmarchelier,[1] E. Hervé,[2,3] F. Brisset,[1] and J.C. Poulin[1]

[1]*ICMMO/LPCES/MAP UMR PSUD-CNRS 8182, Univ. Paris Sud, 91405 Orsay Cedex, France.*
[2]*Université de Versailles, Saint-Quentin en Yvelines,45 Av. des Etats-Unis, F-78035 Versailles Cedex, France*
[3]*MINES ParisTech, Centre des Matériaux, CNRS UMR 7633, BP 87, 91003 Evry Cedex, France*
[*]*Bertrand.poumellec@u-psud.fr*

Abstract: We review the question on the origin of the differences observed on various properties when we scan the femtosecond laser beam in an isotropic media (i.e. a glass) in two orientations of a given direction. Publications on refractive index changes, birefringence, nanogratings, stress, bubbles formation and on quill writing effects are analyzed. A new interpretation based on space-charge built from ponderomotive force and stored in the dielectric inducing an asymmetric stress field is proposed.

OCIS codes: (160.6030) Silica; (320.7130) Ultrafast processes in condensed matter, including semiconductors; (350.3450) Laser-induced chemistry; (320.2250) Femtosecond phenomena.

References and links

1. B. Poumellec, L. Sudrie, M. Franco, B. Prade, and A. Mysyrowicz, "Femtosecond laser irradiation stress induced in pure silica," Opt. Express **11**(9), 1070–1079 (2003).
2. P. Kazansky, W. Yang, E. Bricchi, J. Bovatsek, A. Arai, Y. Shimotsuma, K. Miura, and K. Hirao, ""Quill" writing with ultrashort light pulses in transparent materials," Appl. Phys. Lett. **90**(15), 151120 (2007).
3. M. Gecevičius, M. Beresna, J. Zhang, W. Yang, H. Takebe, and P. G. Kazansky, "Extraordinary anisotropy of ultrafast laser writing in glass," Opt. Express **21**(4), 3959–3968 (2013).
4. P. G. Kazansky and M. Beresna, "Quill and Nonreciprocal Ultrafast Laser Writing," in *Femtosecond Laser Micromachining* (Springer, 2012), pp. 127–151.
5. W. Yang, P. G. Kazansky, Y. Shimotsuma, M. Sakakura, K. Miura, and K. Hirao, "Ultrashort-pulse laser calligraphy," Appl. Phys. Lett. **93**(17), 171109 (2008).
6. Y. Bellouard and M. O. Hongler, "Femtosecond-laser generation of self-organized bubble patterns in fused silica," Opt. Express **19**(7), 6807–6821 (2011).
7. E. Bricchi, B. G. Klappauf, and P. G. Kazansky, "Form birefringence and negative index change created by femtosecond direct writing in transparent materials," Opt. Lett. **29**(1), 119–121 (2004).
8. W. Yang, P. G. Kazansky, and Y. P. Svirko, "Non-reciprocal ultrafast laser writing," Nat. Photonics **2**(2), 99–104 (2008).
9. M. Lancry, N. Groothoff, B. Poumellec, S. Guizard, N. Fedorov, and J. Canning, "Time-resolved plasma measurements in Ge-doped silica exposed to infrared femtosecond laser," Phys. Rev. B **84**(24), 245103 (2011).
10. D. N. Vitek, E. Block, Y. Bellouard, D. E. Adams, S. Backus, D. Kleinfeld, C. G. Durfee, and J. A. Squier, "Spatio-temporally focused femtosecond laser pulses for nonreciprocal writing in optically transparent materials," Opt. Express **18**(24), 24673–24678 (2010).
11. P. Salter and M. Booth, "Dynamic control of directional asymmetry observed in ultrafast laser direct writing," Appl. Phys. Lett. **101**(14), 141109 (2012).
12. P. Salter, R. Simmonds, and M. Booth, "Adaptive control of pulse front tilt, the quill effect, and directional ultrafast laser writing," in *Frontiers in Ultrafast Optics* (International Society for Optics and Photonics, 2013), 861111.
13. K. M. Davis, K. Miura, N. Sugimoto, and K. Hirao, "Writing waveguides in glass with a femtosecond laser," Opt. Lett. **21**(21), 1729–1731 (1996).
14. L. Sudrie, M. Franco, B. Prade, and A. Mysyrowicz, "Writing of permanent birefringent microlayers in bulk fused silica with femtosecond laser pulses," Opt. Commun. **171**(4-6), 279–284 (1999).
15. B. Poumellec, M. Lancry, A. Chahid-Erraji, and P. Kazansky, "Modification thresholds in femtosecond laser processing of pure silica: review of dependencies on laser parameters [Invited]," Opt. Mater. Express **1**(4), 766–782 (2011).
16. J. Canning, M. Lancry, K. Cook, A. Weickman, F. Brisset, and B. Poumellec, "Anatomy of a femtosecond laser processed silica waveguide [Invited]," Opt. Mater. Express **1**(5), 998–1008 (2011).
17. M. Lancry, B. Poumellec, J. Canning, K. Cook, J. Poulin, and F. Brisset, "Ultrafast nanoporous silica formation driven by femtosecond laser irradiation," Laser & Photonics Reviews. In Press.

#191323 - $15.00 USD Received 31 May 2013; revised 1 Aug 2013; accepted 21 Aug 2013; published 3 Sep 2013

18. S. Richter, A. Plech, M. Steinert, M. Heinrich, S. Doering, F. Zimmermann, U. Peschel, E. B. Kley, A. Tünnermann, and S. Nolte, "On the fundamental structure of femtosecond laser-induced nanogratings," Laser & Photonics Reviews **6**(6), 787–792 (2012).
19. C. Hnatovsky, R. Taylor, E. Simova, P. Rajeev, D. Rayner, V. Bhardwaj, and P. Corkum, "Fabrication of microchannels in glass using focused femtosecond laser radiation and selective chemical etching," Appl. Phys., A Mater. Sci. Process. **84**(1-2), 47–61 (2006).
20. M. Beresna and P. G. Kazansky, "Polarization diffraction grating produced by femtosecond laser nanostructuring in glass," Opt. Lett. **35**(10), 1662–1664 (2010).
21. S. Richter, M. Heinrich, S. Döring, A. Tünnermann, S. Nolte, and U. Peschel, "Nanogratings in fused silica: Formation, control, and applications," J. Laser Appl. **24**(4), 042008 (2012).
22. B. Poumellec, M. Lancry, J. C. Poulin, and S. Ani-Joseph, "Non reciprocal writing and chirality in femtosecond laser irradiated silica," Opt. Express **16**(22), 18354–18361 (2008).
23. C. Fan, B. Poumellec, H. Zeng, R. Desmarchelier, B. Bourguignon, G. Chen, and M. Lancry, "Gold Nanoparticles Reshaped by Ultrafast Laser Irradiation Inside a Silica-Based Glass, Studied Through Optical Properties," J. Phys. Chem. C **116**(4), 2647–2655 (2012).
24. C. Fan, B. Poumellec, H. Zeng, M. Lancry, W. Yang, B. Bourguignon, and G. Chen, "Directional Writing Dependence of Birefringence in Multicomponent Silica-based Glasses with Ultrashort Laser Irradiation," J. Laser Micro Nanoen **6**(2), 158–163 (2011).
25. P. G. Kazansky, Y. Shimotsuma, M. Sakakura, M. Beresna, M. Gecevičius, Y. Svirko, S. Akturk, J. Qiu, K. Miura, and K. Hirao, "Photosensitivity control of an isotropic medium through polarization of light pulses with tilted intensity front," Opt. Express **19**(21), 20657–20664 (2011).
26. S. Matsuo, Y. Umeda, T. Tomita, and S. Hashimoto, "Laser-Scanning Direction Effect in Femtosecond Laser-Assisted Etching," Journal of Laser Micro Nanoengineering **8**(1), 35–38 (2013).
27. C. L. Sones, S. Mailis, W. S. Brocklesby, R. W. Eason, and J. R. Owen, "Differential etch rates in z-cut LiNbO3 for variable HF/HNO3 concentrations," J. Mater. Chem. **12**(2), 295–298 (2002).
28. J. Choi, M. Bellec, A. Royon, K. Bourhis, G. Papon, T. Cardinal, L. Canioni, and M. Richardson, "Three-dimensional direct femtosecond laser writing of second-order nonlinearities in glass," Opt. Lett. **37**(6), 1029–1031 (2012).
29. S. Mao, F. Quéré, S. Guizard, X. Mao, R. Russo, G. Petite, and P. Martin, "Dynamics of femtosecond laser interactions with dielectrics," Appl. Phys., A Mater. Sci. Process. **79**, 1695–1709 (2004).
30. D. Bethune, "Optical second-harmonic generation in atomic vapors with focused beams," Phys. Rev. A **23**(6), 3139–3151 (1981).
31. M. Lancry, E. Régnier, and B. Poumellec, "Fictive temperature in silica-based glasses and its application to optical fiber manufacturing," Prog. Mater. Sci. **57**(1), 63–94 (2012).
32. M. Lancry, N. Groothoff, S. Guizard, W. Yang, B. Poumellec, P. Kazansky, and J. Canning, "Femtosecond laser direct processing in wet and dry silica glass," J. Non-Cryst. Solids **355**(18-21), 1057–1061 (2009).
33. F. Quéré, S. Guizard, and P. Martin, "Time-resolved study of laser-induced breakdown in dielectrics," EPL **56**(1), 138–144 (2001) (Europhysics Letters).
34. G. A. Maugin, *Continuum Mechanics of Electromagnetic Solids*, Applied Mathematics and Mechanics (North-Holland Amsterdam, 1988), Vol. 33.

1. Introduction

The Asymmetric Orientational Writing (AOW) is something observed with femtosecond (fs) or picosecond (ps) laser not with nanosecond laser nor continuous ones. It is related to the permanent modification of material under irradiation that is different when one moves the focused laser beam in one sense and the other one. This has been reported for the first time in 2003 in pure silica on the induced stress [1] and then in 2007 on several properties: the index change, the macroscopic texture of the written lines [2], the nanostructures called nanogratings [2]. About the texture of the written line, if you look at the irradiated sample in transmission through an optical microscope, you will discover (if irradiation conditions are suitable) aligned asymmetric macroscopic damages like quarters of moon or chevron like structure that change of orientation under the laser beam displacement [3]. You can also observed bubbles or pearls produced in only one orientation [4, 5] or distributed differently according to the scanning orientation [6]. Pushing a bit the analysis, placing the sample between crossed polarizers, you will notice (again if suitable conditions are fulfilled) that only one orientation is birefringent or that the brightness of lines is different [2]. Kazansky et al. who related the strong birefringence to form birefringence due to the appearance of nanogratings [7] looked at those nanostructures by SEM after chemical etching and found a different texture [2]. On the other hand, on our side, we reported in 2003 [1] shear stress that changes of sign under writing sense reversal. This phenomenon appeared surprising because the glass is isotropic and the beam arriving perpendicularly to the sample face was believed at that time to be axisymmetric.

#191323 - $15.00 USD Received 31 May 2013; revised 1 Aug 2013; accepted 21 Aug 2013; published 3 Sep 2013

Later on, Kazansky et al. [8] suggested that the laser beam symmetry is in fact broken due to a Pulse Front Tilt (PFT) that is inherent to such type of ultrashort pulse laser. This produces an effect similar on the quasi-free electrons to a snow-plough through a term occurring in the ponderomotive force i.e. $-\vec{\nabla}I$ where I is the intensity of the beam in the focal volume. In the same time, Kazansky called that the "Quill" writing [2]. As we can see with the equations below, for short time, the ponderomotive force induced a movement of electrons initially at rest in the direction of $-\vec{\nabla}I$ and then an electronic current in the same direction.

$\vec{J}_e = n_e \vec{v}$ (assuming that the ions are not moving), $\frac{\partial n_e}{\partial t} + div\left(n_e \vec{v}\right) = source - well$, $\frac{\partial \vec{v}}{\partial t} + \left(\vec{v}\vec{\nabla}\right)\vec{v} = \frac{\text{ponderomotive force}}{n_e}$, the term "sources" account for by multiphoton ionization or tunnelling and/or avalanche ionization and the term "wells" is for electron trapping under self trapped excitons [9]. The electronic current induces an electric and a heat current that are generally different in a non-centersymmetric crystal like $LiNbO_3$. This term is invoked for producing asymmetric heating in [8]. In that case, a PFT is not necessary, in contrast to what occurs in glasses.

Because the PFT was suggested to be at the root of the symmetry breaking, several groups made efforts to prove it. A first experiment was performed by reversing the beam spatial symmetry by introducing an additional mirror on the optical path and actually they reversed the observation [5]. This proved that the asymmetry originates actually in the beam. But the most clearcut proof has been given by Vitek et al. [10] making a special set-up for controlling the PFT at will. Let us mention here on the way, that they increased the PFT by more than 5 order of magnitude but they do not observed a change of AOW in the same proportion. More recently, Salter et al. [11, 12] used a SLM (Spatial Light Modulator), a less costly system and more flexible one, for suppressing or reversing the AOW easily by controlling the PFT. They show also that PFT is not necessary for AOW, just an intensity gradient without PFT is able to produce it. Therefore, we can deduce that asymmetry in the plasma density is required for AOW but why it is not observed for any set of laser parameters? For getting an insight on these conditions, as the properties exhibiting AOW are various, let us study them in details.

2. Results

Let us start with the refractive index permanent change [13]. As the pulse energy is increased, it is now widely known that above a first energy threshold (T1), the index change is almost isotropic (with only a small birefringent contribution from form stress). Then going on increasing the energy, a second threshold is overcome (T2) and a strong negative birefringence appears [14]. These processing windows have been recently reviewed in ref [15]. This negative birefringence has been attributed to the appearance of nanostructures also called nanogratings [7]. We can see a nice example of such a nanostructure in Fig. 1 that shows secondary electrons images of laser track cross-section for lines written in opposite orientations. It is series of nanoplanes that we proved to be decomposed silica (i.e. nanoporous silica containing molecular oxygen) [16, 17]. This has been confirmed recently in Ref [18]. They are sometimes well organized like with Fig. 1, sometimes more disordered (especially at higher pulse energy [19]).

We have decided to study the retardance (proportional to the birefringence) and the nanostructures systematically in order to check if they are correlated. In first, we detected that changing the sense of writing for the configuration used in Fig. 1 i.e. Xy (writing horizontal i.e. X, laser polarization vertical i.e. y), the length of the laser tracks and thus the length of the volume containing the nanostructures varies. On the contrary, the number of nanoplanes transversally remains the same. Looking the birefringence at the cross section of the sample by transmission between crossed polarizers correlate to the observed change on the nanostructures.

#191323 - $15.00 USD Received 31 May 2013; revised 1 Aug 2013; accepted 21 Aug 2013; published 3 Sep 2013

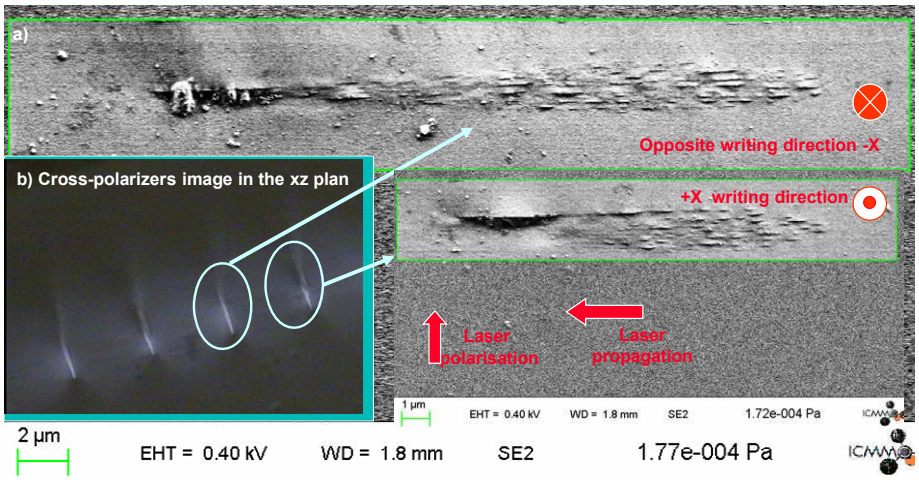

Fig. 1. FEG-SEM, Secondary electrons images of the cross-section of laser tracks written in opposite orientation. The laser parameters were: 0.4 µJ/pulse, 800 nm, 160 fs, 200 kHz, 0.5 NA, 100 µm/s i.e. 2.10^3 pulses/µm. (b) Cross-section microscope images taken between crossed polarizers with the birefringent lines slow axis oriented at about 30° of the polarizer.

Quantitatively, the retardance changes from 110nm (+ X scanning) to 150nm (-X scanning) for perpendicular configuration (see Fig. 2(b)). This seems to be smaller than the value that we can expect from Fig. 1 as the retardance is proportional to the length, the number of nanoplanes and increases with the refractive index difference between the matter within the nanoplanes (i.e. nanoporous silica) and the matter between them, but one has also to take into consideration the size of the probe beam used for performing the measurement with respect to the laser track width. That is why, in order to minimize any misinterpretation, we used QPM (Quantitative Phase Measurements) and Abrio (Quantitative retardance measurements) for performing a correct correlation between retardance and nanostructures, by varying the laser parameters. We first measured the profiles of phase, retardance and slow axis orientation (this will be reported extensively in another paper). From this database, we were able to plot the Fig. 2 including the phase change and the retardance for the two orientations (+ X and –X) for two different configurations i.e. Xx and Xy. As it is well known, we see on the phase curve that whatever the configuration (but not for the same energy range), there is an increase of the average index change (above T1 threshold) followed by a strong decrease above T2 threshold. It is important to note that the phase and thus the azimuthal average index exhibit an orientational asymmetry. It is larger on Xx than on Xy configuration.

#191323 - $15.00 USD Received 31 May 2013; revised 1 Aug 2013; accepted 21 Aug 2013; published 3 Sep 2013

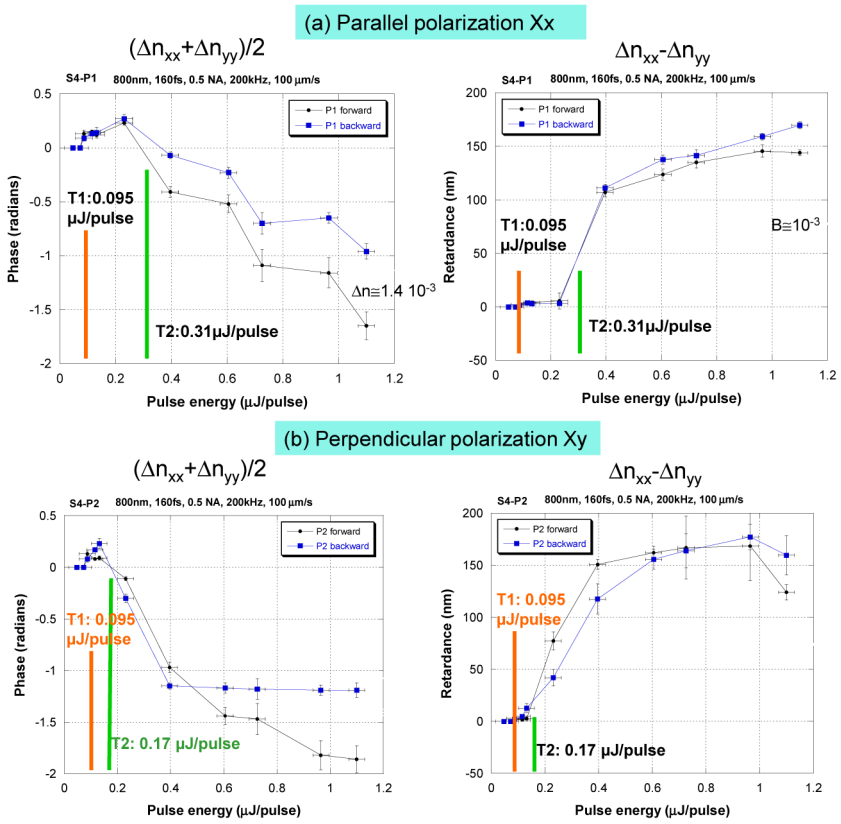

Fig. 2. Plot of the quantitative phase Δφ (left side) and retardation (right side) with respect to writing velocity in left-to-right (+ X) direction (blue squares) and right-to-left (-X) direction (black squares). The pulse energy was varied from 0.05 up to 1.1 µJ/pulse. (a) parallel polarization quoted Xx; (b) perpendicular polarization quoted Xy. T1 and T2 thresholds are shown by arrows. The other laser parameters were: 800 nm, 160 fs, 200 kHz, 0.5 NA, 100 µm/s i.e. 2.10^3 pulses/µm.

Asymmetry is also detected on retardance profiles across the lines as shown in Fig. 3. This has been mentioned previously by Beresna et al. [20]. The authors observed retardance amplitude that is larger on one edge of the line when they write in one sense or the other one but they did not quantify it. In Fig. 3, we see that for Xy configuration (Left plot), the magnitude of the retardance changes on the sense of writing whereas for Xx configuration (Right plot), the retardance does not change in magnitude but is transversally asymmetric.

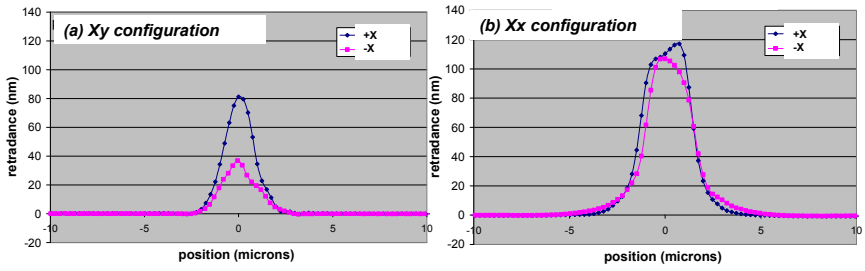

Fig. 3. Plot of the retardance profile with respect to writing velocity in left-to-right (+ X) direction (blue squares) and right-to-left (-X) direction (pink squares). (a) Perpendicular configuration quoted Xy, (b) parallel configuration quoted Xx. The laser parameters were: 0.4 µJ/pulse, 800 nm, 160 fs, 200 kHz, 0.5 NA, 100 µm/s i.e. 2.10^3 pulses/µm.

#191323 - $15.00 USD Received 31 May 2013; revised 1 Aug 2013; accepted 21 Aug 2013; published 3 Sep 2013

We can now correlate these asymmetries according to the laser pulse energy (Fig. 4). We see in this figure that no AOW appears on retardance for low energies but for higher energy around 0.7 µJ. With the writing conditions used here, the difference with the sense of writing is quite spectacular (jumping from 100 down to 40 nm) and can have a negative impact on the writing technology, clearly. Trying to see what are the corresponding changes on nanostructures, we cleaved the sample and observed the cross section using SEM as shown at the right side of Fig. 4. When no AOW is detected on retardance, there is nevertheless a transversal asymmetry on the nanostructures that reverses under the sense of writing. We can deduce that it is an antisymmetric orientational writing. Increasing pulse energies, leads to the increase not only of the length of the nanostructures but also of the number of nanoplanes. At 0.6 µJ, whereas no AOW is detected on retardance, there is already a dissymmetry on the number of nanoplanes.

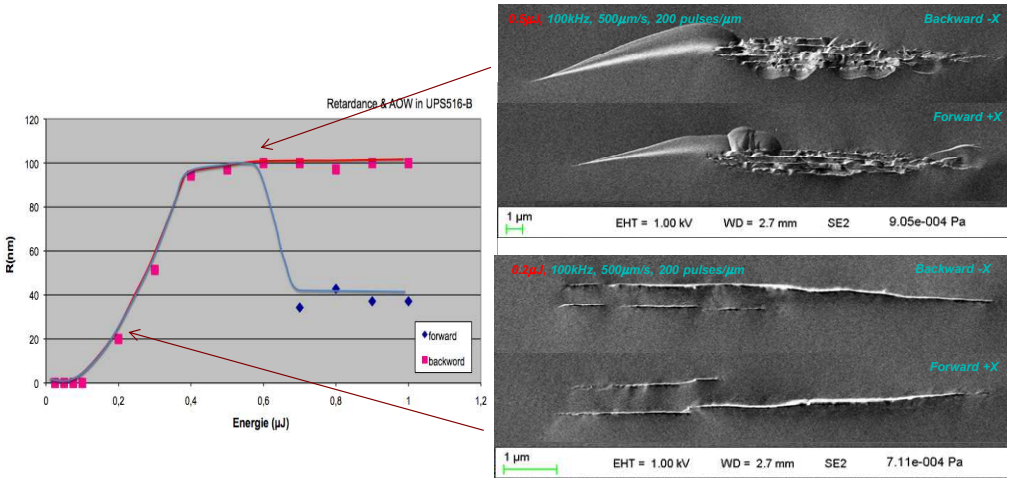

Fig. 4. (Left) Plot of retardance according to the laser pulse energy with respect to writing velocity in left-to-right (+ X) direction (blue squares) and right-to-left (-X) direction (pink squares). The pulse energy was varied from 0.025 up to 1 µJ/pulse. The laser polarization was perpendicular Xy. The other laser parameters were: 1030 nm, 300 fs, 100 kHz, 0.5 NA, 500 µm/s i.e. 200 pulses/µm. (Right) FEG-SEM, Secondary electrons images of the cross-section of laser tracks for writing laser polarization perpendicular to the scanning direction.

Nevertheless, in another sample, varying the energy, we were able to correlate the retardance and the nanograting length whatever the configuration may be. This is shown in Fig. 5. The quality of the linear fit leads us to consider that the retardance is proportional to the nanostructure length (i.e. in the z propagation direction). As we have seen in Fig. 4 that the number of nanoplanes (i.e. laser track width) increases also with increasing energy in the low energy range, this indicates that the retardance is also proportional to the number of nanoplanes within the probe volume.

#191323 - $15.00 USD Received 31 May 2013; revised 1 Aug 2013; accepted 21 Aug 2013; published 3 Sep 2013

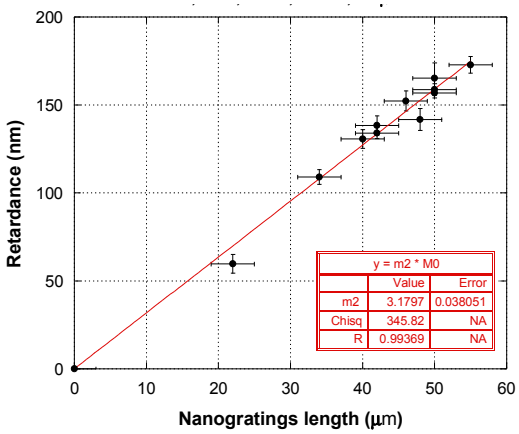

Fig. 5. Plot of retardance according to the nanogratings length (in the z propagation direction). The pulse energy was varied from 0.4 up to 1.2 µJ/pulse. The laser polarization was perpendicular Xy. The other laser parameters were: 800 nm, 160 fs, 200 kHz, 0.6 NA, 200 µm/s.

The next question is the dependence on the beam scanning speed. As the movement is inherent of the AOW, is it obtained for any speed? For answering, we have measured the retardance for 10 to close to 10^3µm/s (see Fig. 6). As it can be seen in Fig. 6, the retardance exhibits AOW for speed lower than 500 µm/s (i.e. more than 200pulses/µm). Looking at the nanostructures, we can see as before that the number of nanoplanes appears the same for 200µm/s (i.e. 500 pulses/µm) when the orientation of writing is changed whereas AOW on retardance is clearly detected. This is surprising considering the form birefringence model and the observation we made according to the pulse energy. Our knowledge on the nanograting structure is therefore to be completed. It is likely that the index difference between the nanoplanes and the surrounding matter, also changes.

When the speed is increased, AOW on retardance vanishes but difference on nanostructure is detected. This corroborates that the structure of nanogratings changes according to the number of pulses per µm for a fixed pulse energy. By the way, as shown by Taylor and Corkum groups [19] and by Nolte group [21], 10-100 pulses/µm are necessary for appearance of nanoplanes organisation. It is worth noticing that if the writing speed affects the modification, this means that a cumulative effect works. This can occurs only through a memory process or when the previous modification is not erased by the next pulses.

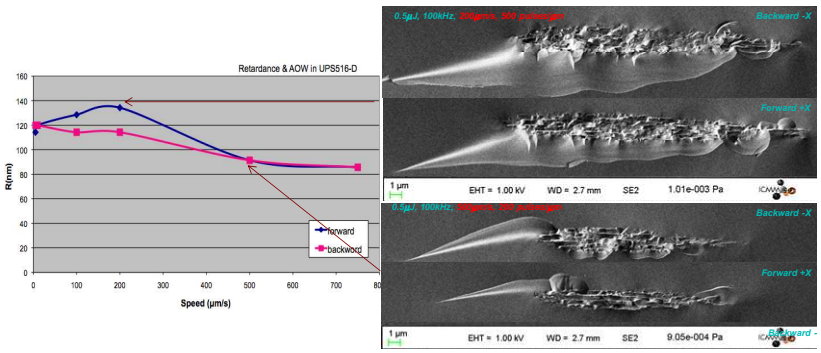

Fig. 6. (Left) Plot of retardance according to the laser writing speed with respect to writing velocity in left-to-right (+ X) direction (blue squares) and right-to-left (-X) direction (pink squares). The pulse energy was fixed to 0.5 µJ/pulse. The laser polarization was perpendicular Xy. The other laser parameters were: 1030 nm, 300 fs, 100 kHz, 0.5 NA. (Right) FEG-SEM, Secondary electrons images of the cross-section of laser tracks for writing laser polarization perpendicular to the scanning direction.

#191323 - $15.00 USD Received 31 May 2013; revised 1 Aug 2013; accepted 21 Aug 2013; published 3 Sep 2013

On the other hand, the effect of the repetition rate on the energy threshold for the appearance of the AOW seems relatively weak varying only from 0.5 µJ to 0.8µJ when the repetition rate is decreased from 500 kHz down to 5 kHz but with a speed of hundred's µm/s. On the contrary, the sensitivity of AOW energy threshold is much larger for a repetition rate of 1 kHz when the scanning speed is increased from 10 to 1500 µm/s (blue curve in Fig. 7 on the left). This leads to consider that the relevant parameter is the number of pulses per µm or the overlap ratio between pulses i.e. 1-v/(f.D), where v is the scanning speed, f the repetition rate and D the beam diameter at the focus. Results plotted in Fig. 6 shows that even with an overlap ratio as low as 0.5, it is still possible to observe AOW for pulse energy larger than 1.8 µJ with the laser condition that we used here.

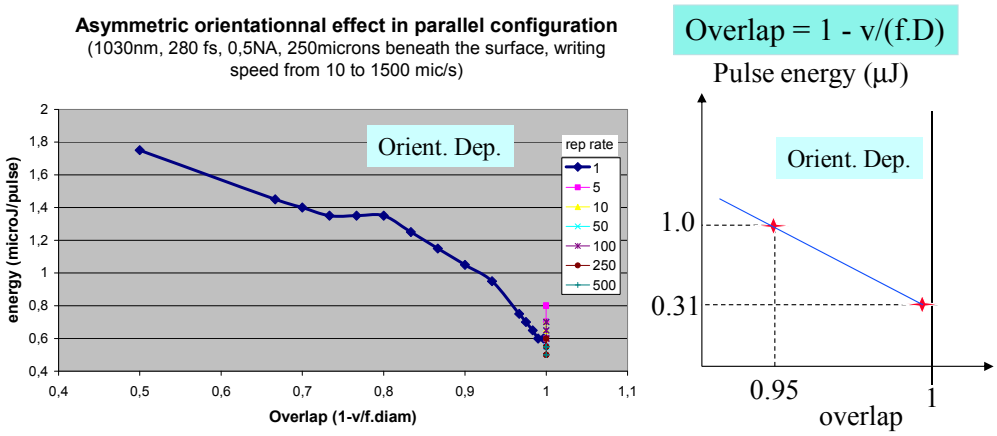

Fig. 7. (Left) Plot of the AOW threshold pulse energy according to the pulse to pulse overlap ratio. The overlap ratio between two consecutive pulses is defined by 1-v/(f.D), where v is the scanning speed, f the repetition rate and D the beam diameter at the focus. The repetition rate was varied from 1kHz up to 500kHz and the scanning speed from 10 up to 1500µm/s. The other laser parameters were: 1030 nm, 300 fs, 0.5 NA, parallel polarization Xx. (Right) The laser parameters were 800nm, 130fs, 1kHz, 0.6NA.

We have mentioned at the beginning that AOW is not only observed on the refractive index change but also on residual stress field due to irradiation. This phenomenon has been extensively described in two papers [1, 22]. We have just to recall here that it is a complex effect when the pulse energy falls in the domain where the nanostructures are formed in pure silica (above T2 threshold). In that case, one possibility for explaining the observed AFM topography shown in Fig. 8 may be a shear solicitation which direction is along the direction of writing. Taking into account the direction of propagation of the laser light, shearing is like a scissor and reveals a chiral action. There are two kinds of shearings: one with a given chiral type and the mirrored one. What we observe, looking at the cross section of the laser tracks, is that there are successive shearings of opposite sign along the laser track. The most striking feature is that shearing around the focal volume is sensitive to the orientation of writing and to the laser polarization direction. It can reverse with the orientation or just change in amplitude. On the contrary, shearing close to the filament, is not sensitive to the orientation of writing nor to the laser polarization direction.

From these results, we can imagine that the stress field sensitive to AOW is related to nanostructures but this is not the case. In Fig. 8, we show a comparison of AFM topography (that reveal the displacement field due to strain relaxation after cleaving the sample) and SEM image in secondary electrons of two lines written in opposite orientation. There are no nanogratings, just a line around which a pair of shearings is clearly visible. The AOW appears here on the length of the laser track which is seen as a very thin structure. We see also that the displacement field changes. This shows clearly that the shearing is associated with AOW. This stress fields impact the refractive index change through photoelastic effect resulting in anisotropic index changes. As shown in Fig. 3, AOW appears on the retardance amplitude but

#191323 - $15.00 USD Received 31 May 2013; revised 1 Aug 2013; accepted 21 Aug 2013; published 3 Sep 2013

also on its slow axis direction. The first quantity change is due to the change in the length of the line. The second quantity shows that the slow axis departs from the direction of the lines due to the effect of the shear stress. The fact we obtain AOW without series of nanoplanes (i.e. below T2 threshold) is consistent with the possibility to observe it in other glasses.

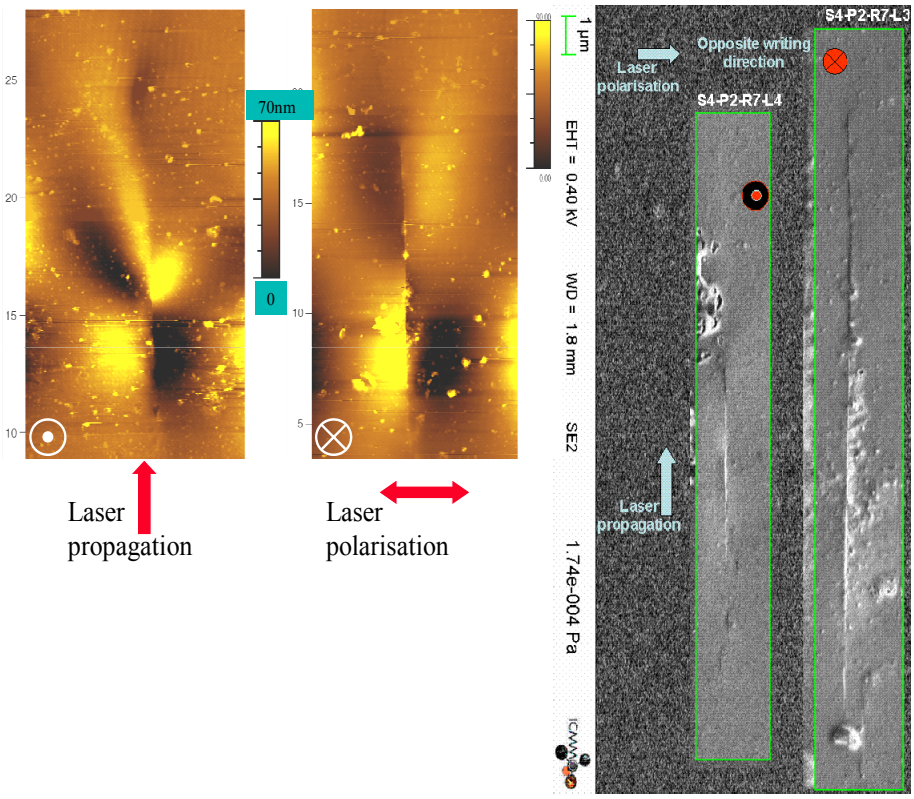

Fig. 8. (Left) Two laser traces written in opposite directions (+ X and –X) seen in AFM after cleaving the sample. The contrast is topographic. The laser is coming from the bottom. The laser parameters were: 0.23 µJ/pulse, 800 nm, 160 fs, 200 kHz, 0.5 NA, 100 µm/s i.e. 2.10^3 pulses/µm. The laser polarization was perpendicular to the scanning direction. (Right) FEG-SEM, Secondary electrons images of the cross-section of the same laser tracks written in opposite directions.

As a matter of fact, we observe it in soda lime silicate [23], in Li_2O-Nb_2O_5-SiO_2 [24]. Other authors reported AOW in alumino-borate [4, 5], and in chalcogenide glasses [3]. Let us report what we have observed in Li_2O-Nb_2O_5-SiO_2 glasses (see Fig. 9). The measurements of the retardance in this kind of glasses is shown in Fig. 9 for four possible configurations of writing direction and polarization varying the scanning speed from 10 µm/s up to 500 µm/s. From each of them, the sense of writing has been investigated. As we can see, AOW is detected for three of them, vanishing for large speed, whereas the retardance is not decreasing. This confirms that the overlap should be larger than a certain value to observe AOW as we saw in Fig. 7. On the contrary, the average retardance value is weakly dependent on the scanning speed as shown in Fig. 6 which was for a pure silica glass. A surprising feature in Fig. 9 is the absence of AOW for the configuration Yy. The idea that AOW is determined by only the PFT would lead to say that it was detected for any laser configuration, not perpendicular to the PFT [4, 25]. This would imply that if no AOW appears for Yy, there should be no AOW also on Yx but this is actually not the case. Clearly, the laser polarization plays a role in the phenomenon. In addition, we measured the PFT and found it is oriented 36° anticlockwise in the xy plane and 0.064° out of the z axis for a 5mm wide beam (i.e.

#191323 - $15.00 USD Received 31 May 2013; revised 1 Aug 2013; accepted 21 Aug 2013; published 3 Sep 2013

before focusing). The explanation of our results is thus not straightforward with the theory available. Lastly, it is worth mentioning that birefringence is produced in this sample by stress field.

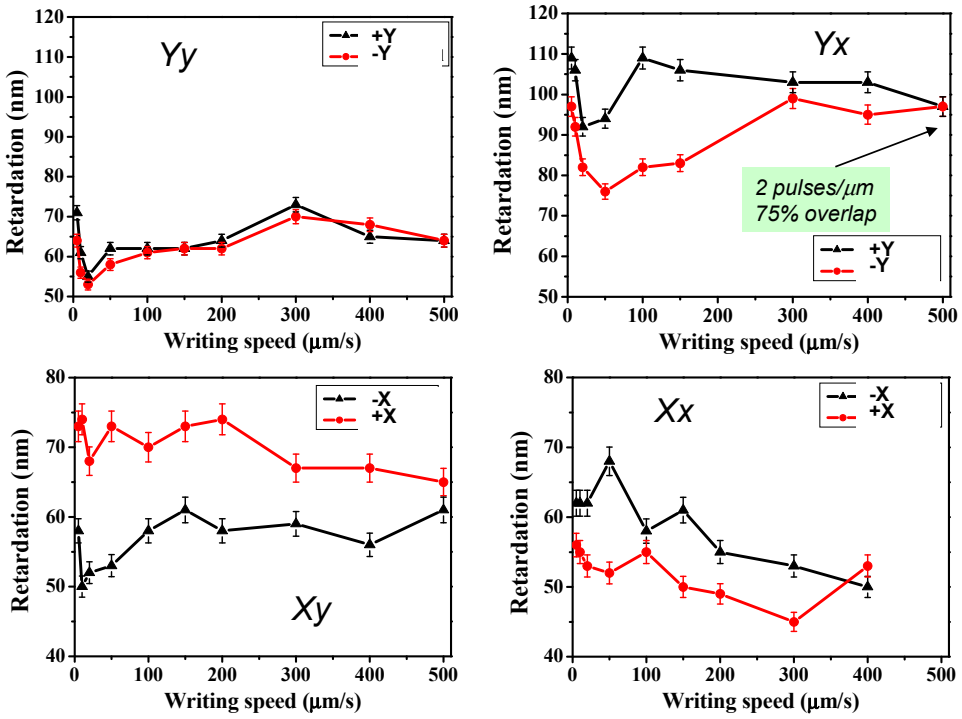

Fig. 9. (Upper part) Plot of the retardation with respect to writing velocity in + Y direction (black triangles) and -Y direction (red dots): (a) parallel polarization Yy; (b) perpendicular polarization Yx. (Bottom part) Plot of the retardation with respect to writing velocity in + X direction (red dots) and -X direction (black triangles): (c) perpendicular polarization Xy; (d) parallel polarization Xx. The other laser parameters were: 2.3 µJ/pulse, 800 nm, 120 fs, 10 kHz, 0.5 NA.

An interesting experiment related to the impact of stress is reported in Genevicius et al. [3]. These authors have studied the variation of retardance with the distance that separates the neighbouring lines written in the same direction and orientation. The resulting retardance increases linearly when the distance between adjacent lines is reduced from 3 down to 0.5µm whereas in the case of superimposition, it should be proportional to the number of lines in the probe focus i.e. a hyperbolic function of the separation distance. We can thus deduce that the stress from the previously written line influences the modification of the next line resulting in a reduced stress field and related retardance. These authors show also that the modification in the front of the written lines is influenced by the stress produced by the previously written lines. This means that the effect of the pre-existing stress field is not only on the magnitude of the modification but is also "tensorial".

Another suspicion of asymmetry is revealed by the same group in [25] in an Aluminoborosilicate glass without movement but with an accumulation of a large number of pulses. They show the production of bubbles in one side of the interaction volume when the polarization is almost horizontal. Their explanation is related to the effect of a heat current with such an expression: $\vec{J} = -\zeta \vec{E}\left(\vec{E}.\frac{\vec{\nabla} n_e}{n_e}\right)$ where n_e is the quasi-free electron density, ζ is a scalar coefficient. In this flux, $\vec{\nabla} n_e$ is produced by the PFT and thus oriented in its direction. Therefore, the current is maximal when laser polarization and PFT makes the smaller angle,

#191323 - $15.00 USD Received 31 May 2013; revised 1 Aug 2013; accepted 21 Aug 2013; published 3 Sep 2013

and zero when the polarization is in the PFT plane. This explanation seems to be in agreement with the symmetry of the observation but they detect also a halo around the interaction volume which is being probably related to heat diffusion which does not exhibit any asymmetry. We can think thus that the vectorial combination suggested is correct but the heat current is not the basis of the bubble production. Rather a charge current may be proposed.

As a matter of fact, in a recent paper [26] some authors describe a pertinent experiment that may be related to electronic polarization of isotropic matter i.e. pure silica. They show that when lines is written in some directions from one end to the other one of a sample, the chemical etching rate is not the same from one face or from the other one. This difference is observed maximum horizontally. Its sign depends on the pulse energy. It exits for a sufficient overlaps. Such a difference in etching rate has been already described in the past but in polar crystal $LiNbO_3$ [27]. It arises from different chemical reaction due to different surface charge because of permanent electric dipole associated to ferroelectric property of the crystal. It is likely that the same phenomenon occurs for irradiated fused silica and reveals thus that permanent polarization has been produced in volume. However, as pure silica does not contain ferroelectric matter, we can say that a space charge is built along the written line. We have engaged measurements with electrostatic force microscope and preliminary results seem to confirm this remark. Such a charge migration is also invoked in silver diffusion in [28] explaining the spatial structure of the SHG source. We can think that this space charge is the consequence of electron migration produced by the ponderomotive force i.e. by $\vec{\nabla} I$ when this one exhibits a net transverse component.

A decisive experiment on that point is the one from Salter et al. in 2012 [11, 12]. These authors using a SLM (spatial light modulator) produced on one hand PFT of different sign and observed a reversal of AOW but they built also a transversally asymmetric intensity gradient without PFT and produced the same effect in fused silica showing that the gradient intensity is at the basis of the process.

3. Tentative mechanism

Our proposal for symmetry breaking will be therefore based on the above review and results. In the condition that we used for inducing permanent refractive index change, the plasma is formed by multiphoton ionization (or by tunneling) in a few 10's of fs above an energy threshold and in the same time it is heated by multiphoton absorption of the excited electrons in the conduction bands. If impact ionization plays a role in the excitation for higher energy density, it does not change the view. One hundred femtosecond later, a part of the excited electrons couple with the phonons and stabilize under Self Trapped Excitons (STE) below the bottom of the conduction band [9, 29]. Notice that STE formation is specific to some glassy materials like silica and doped-silica but not all of them. In the first part of this process, electrons are mobile and moves under the ponderomotive force as described by Bethune [30]. The plasma becomes transversally asymmetric (Bethune discussed the timescale for such process and the conditions are actually fulfilled in our case). Since STE's are almost immobile, they will "record" the non-uniformity of the plasma spatial distribution that will survive after the pulse will be exhausted. Then, STE's relaxe (their lifetime is less than a few 100's ps at room temperature) and a space charge is definitely stored in the matter (this space charge is a separated charge of opposite sign, it is globally neutral). However, we can note that in the same time, the matter temperature increases in a few 10's ps and will decrease down to room temperature by thermal diffusion at the scale of one μs. With the typical pulse energy and the repetition rate that we used (below 500 kHz), pulses are thus completely separated and there is no heat accumulation from pulse to pulse. The space charge in a hot matter can deform the matter thanks to the opposite charge attraction. Nevertheless, the time is not long enough, considering the atomic mobility to completely erase the space charge by ionic migration or plastic deformation. When the matter has returned to room temperature, it contained therefore a space charge, a plastically deformed matter and a stress field due to

#191323 - $15.00 USD Received 31 May 2013; revised 1 Aug 2013; accepted 21 Aug 2013; published 3 Sep 2013

residual electrostatic force and modification of mechanical properties due to the irradiation (in particular fictive temperature [31] that increases after laser irradiation [15]).

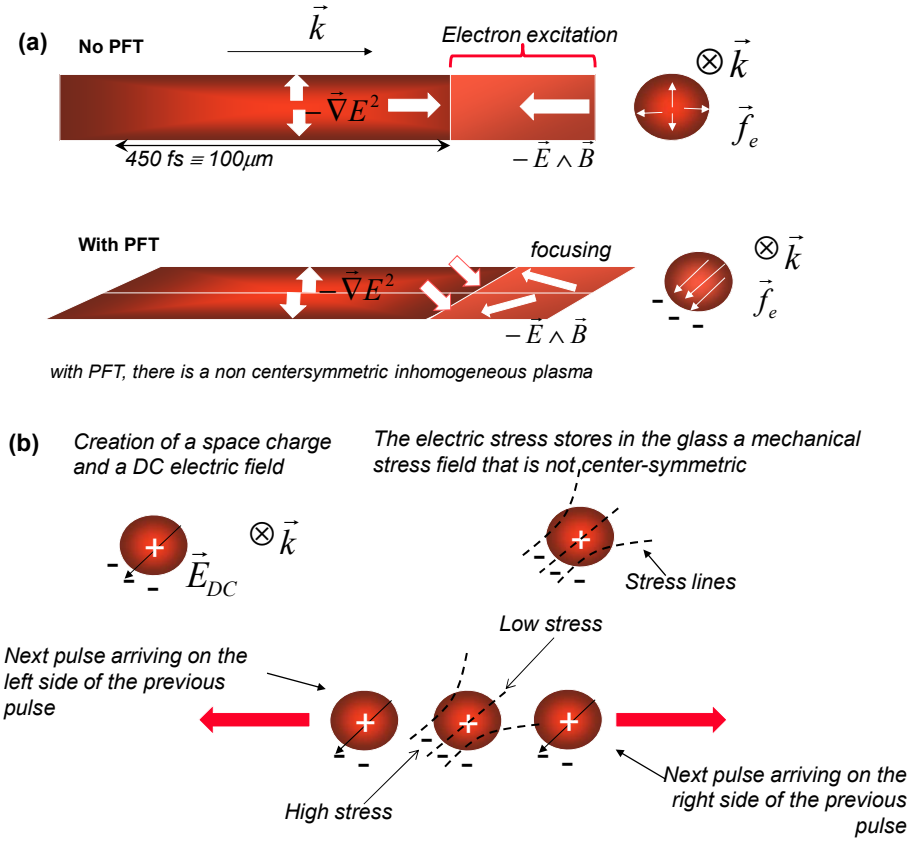

Fig. 10. Tentative mechanism and related phenomena to illustrate the appearance of AOW. The drawing in red symbolizes the laser pulse spatial extent

Figure 10 tries to illustrate the appearance of AOW based on this scheme. The expression of the time averaged part of the ponderomotive force just after the creation of the plasma is the following considering static electron plasma:

$$\vec{f}_e = \left(\vec{P}_e \bullet \vec{\nabla}\right)\vec{E} + \frac{\partial \vec{P}_e}{\partial t}\wedge\vec{B} = \varepsilon_0 \chi_{fe}\left(\frac{\vec{\nabla}\vec{E}^2}{2} + \frac{\partial\left(\vec{E}\wedge\vec{B}\right)}{\partial t} + \frac{\partial n_e}{n_e \partial t}\vec{E}\wedge\vec{B}\right) \quad \text{where}$$

$$\vec{P}_e = \varepsilon_0 \chi_{fe}\vec{E} \text{ with } \varepsilon_0 \chi_{fe} = -\frac{n_e e^2}{m\omega^2}.$$

The first term of the last part of the equation is sensitive to the pulse front tilt, it pushes the electrons forward in front and on the edge of the side of the pulse (see Fig. 10a). The second and the third terms are oriented by the Poynting vector; they act partly in the opposite orientation of the first term with the same strength. They push the electrons back to the PFT but they are not sensitive to the PFT. In strong converging regime, they tend to decrease the electron density at the center of the focal volume. The first term in $\vec{\nabla}E^2$ has also a similar effect, more efficient but it introduces a dissymmetry when PFT is not zero. In conclusion, in the absence of a PFT, the electrons are just pushed out from the center whereas with a PFT, they are pushed more on one side. As shown by Bethune [30], this creates a DC field but here without center of symmetry (see Fig. 10b). Lifetime of the electrons may be smaller than the

#191323 - $15.00 USD Received 31 May 2013; revised 1 Aug 2013; accepted 21 Aug 2013; published 3 Sep 2013

pulse duration and part of them are trapped under STE's (typically within 150fs in silica or doped-silica) [9, 32, 33]. A large part of them is readily re-ionized but this does not erase the DC field. A small part of the STE's relaxe over a few 100's ps under charged point defects that contribute to record the electric field into the glass network. Also as the pulse ends, the glass temperature increases. Glass distorts but does not screen the electric field completely because melting is not achieved (time at high temperature is too short). When glass has cooled down again, it contains an electric field, a free of stress deformation (or strain) field and a residual stress field.

As we can see, due to non-centersymmetry of the charge distribution, the stress distribution is not centersymmetric either. Hence, when a next pulse strikes the matter it begins to erase a part of the charge distribution and a part of the stress field but not completely. A part of the previous irradiated matter is not irradiated again and induces a stress field in the next focal volume. As we mentioned above, we believe that this stress field interacts in the transformation process of the matter under irradiation. Therefore, as the stress field is not the same on one side and the other of the previous pulse, the matter transformation may be different as we believe from [25] that the transformation kinetics is sensitive to the stress field. In this scheme, there is only one direction for which AOW cannot be detected; it is when scanning direction is perpendicular to $\vec{\nabla}\vec{E}^2$ or in the plane of the PFT.

In the ponderomotive expression considered until now (when light is on), the laser polarization does not play a role whereas the experiment clearly points out an effect. For getting back in the mechanism a laser polarization effect, we have to relax part of the assumption made until now. The first one can be to consider the appearance of a contribution of the static field in the ponderomotive expression but this does not introduce an effect, the plasma polarization remaining linear. The second possibility is that plasma polarization is no more linear in $\vec{E}$ at the laser frequency. The first non-linear contribution at the laser frequency may be from third order polarization. In isotropic media like plasma is, in the dipolar approximation, we can write $\vec{P}_{NL}^{3D} = \varepsilon_0 \chi_{eff}^{(3d)} |E|^2 \vec{E}$ i.e. a term parallel to the laser polarization that is just modifying χ_{fe} and does not introduce term sensitive to laser polarization in the ponderomotive force. In the quadrupolar approximation, we have:

$$\vec{P}_{NL}^{3Q} = \varepsilon_0 \chi_{eff,1}^{(3q)} |E|^2 \frac{\partial \vec{B}}{\partial t} + \varepsilon_0 \chi_{eff,2}^{(3q)} \left(\vec{E} \wedge \vec{\nabla}\right) |E|^2 \qquad (1)$$

On the contrary to dipolar contribution, this term introduces component dependent on the laser polarization. This is also the case if we relax the third assumption i.e. the electron plasma speed is not negligible. In that case, terms we have to considered is given for example by Maugin [34]. We have:

$$\left(\vec{P}.\vec{\nabla}\right)\left(\vec{v} \wedge \vec{B}\right) + curl\left(\vec{P} \wedge \vec{v}\right) \wedge \vec{B} + div(\vec{P}).\vec{v} \wedge \vec{B} + \left(\vec{\nabla} \times \vec{B}\right)\left(\vec{v} \wedge \vec{P}\right). \qquad (2)$$

It is a bit cumbersome but it can be shown that these terms introduce mostly forces perpendicular to $\vec{\nabla}\vec{E}^2$ and to $\vec{B}$. They deviate all the direction of the plasma density gradient according to the laser polarization. Rough computation of their amplitude considering that average speed allows the electron to cross the beam radius during the pulse duration, shows that they are of comparable order of magnitude when compared to the ponderomotive force at zero speed in our conditions. These two last contributions are thus important for explaining the laser polarization effect in AOW. The larger effect is when the laser polarization lies in the rotation plan of the PFT, increasing its effect.

4. Conclusion

After reviewing the publications together with new results that show AOW on refractive index changes, birefringence, nanogratings, stress, bubble formation, their analyses suggest a

#191323 - $15.00 USD Received 31 May 2013; revised 1 Aug 2013; accepted 21 Aug 2013; published 3 Sep 2013

new interpretation based on a space-charge built from ponderomotive force and stored in the dielectric inducing an asymmetric stress field. With such mechanism, we are able to explain most of the observations. Additional experiments are nevertheless required for establishing definitely the existence of the space charge and the spatial distribution of the stress field. Even though, we do not explain everything at the moment like the shearing inversion on scanning orientation inversion but we are working on considering the spatial distribution of the ponderomotive force that appears when plasma electron speed is not neglected.

Acknowledgments

This work has been performed in the frame of FLAG (Femtosecond Laser Application in Glasses) consortium project with the support of several organisations: the Agence Nationale pour la Recherche (ANR-09-BLAN-0172-01), the RTRA Triangle de la Physique (Réseau Thématique de Recherche Avancée, 2008-056T), the Essonne administrative Department (ASTRE2007), the Ministry of the Foreign Affairs (PHC Alliance) and FP7-PEOPLE-IRSES e-FLAG 247635.

#191323 - $15.00 USD Received 31 May 2013; revised 1 Aug 2013; accepted 21 Aug 2013; published 3 Sep 2013